Bull. Fac. Fish. Hokkaido Univ.
51(1), 31-43, 2000.

Anticyclonic, Baroclinic Eddies along 145°W in the Gulf of Alaska in 1994-1999

Hiroji ONISHI[1), Shintaro OHTSUKA[1) and Gen ANMA[2)

Abstract

The Alaskan Gyre is a large cyclonic gyre in the North Pacific Subarctic Ocean formed from three major current systems (Subarctic Current, Alaska Current and Alaskan Stream). Sectional hydrographic observations in the Gulf of Alaska have been made every summer during 1994-1999 by the T.S. Oshoro-Maru of the Faculty of Fisheries, Hokkaido University. Along 145°W, mesoscale anticyclonic eddies have been observed in every year. They are large (diameter >200 km), deep (to 2,000 m depth) and were observed near the same location each year. The center of the eddies had a low salinity surface layer and a warm core temperature near 100 m depth. These characters are similar to those of coastal waters in the Gulf of Alaska and of the Alaskan Stream water. In each eddy the baroclinic field was very deep, and the geostrophic velocity increased towards the surface. In 1995, the eddy surface speed was over 20 $cm \cdot s^{-1}$ and the volume transport was over $13 \times 10^6\ m^3 \cdot s^{-1}$. These eddies strongly affect the circulation of Alaskan Gyre and presumably influence local fisheries.

Key words: Alaskan Gyre, Baroclinic Eddy, Anticyclonic Eddy, Subarctic Circulation

Introduction

Circulation in the Gulf of Alaska is characterized by the cyclonic Alaskan Gyre (Fig. 1), which consists of the eastward-flowing Subarctic Current at about 50°N, the northward-flowing Alaska Current and the southwestward-flowing Alaskan Stream along the Alaskan Peninsula (Uda, 1963; Dodimead et al., 1963; Favorite et al., 1976; etc.). Using hydrographic data collected from 1927 to 1967, Tabata (1982) showed that anticyclonic eddies occur frequently off Sitka. These eddies (named Sitka Eddy) typically have a diameter of 200-300 km, a deep (>2,000 m) baroclinic structure, a warm core near 200 m depth and a halocline depression. In recent years, satellite data has been used to analyze eddies in the Gulf of Alaska. Matthews et al. (1992) examined the Sitka Eddy from GEOSAT altimetry data and found that the eddy moves westward. Thomson and Gower (1998) found an anticyclonic eddy chain in a coastal area of the Gulf of Alaska using NOAA thermal imagery. Meyers and Basu (1999) pointed out the relation between the amplitude of anticyclonic eddies and ENSO strength using TOPEX/POSEIDON altimetry data. However, there have been few hydrographic studies in this region, especially in the central area of the Gulf of Alaska, so the vertical features of eddies after they move westward into the central gulf are unknown. The present paper is a physical

[1) *Laboratory of Physical Oceanography, Faculty of Fisheries, Hokkaido University*
(北海道大学水産学部物理海洋学講座)
[2) *Training Ship of Oshoro-Maru, Faculty of Fisheries, Hokkaido University*
(北海道大学水産学部練習船おしょろ丸)

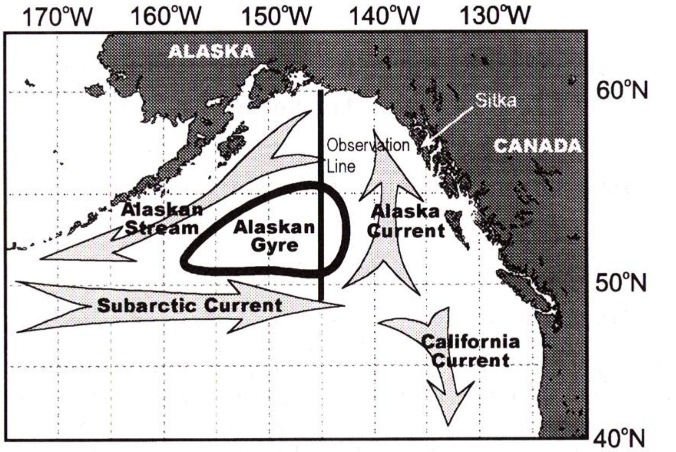

Fig. 1. Schematic diagram of the surface circulation in the Gulf of Alaska.

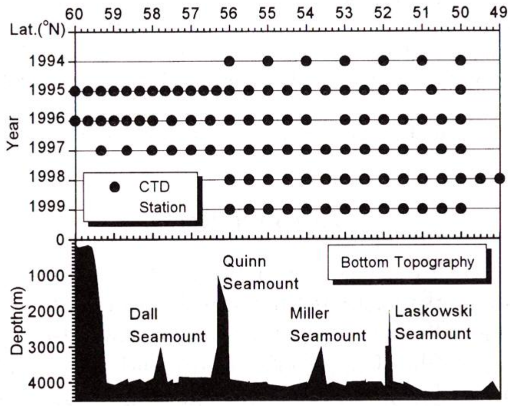

Fig. 2. CTD observation points from 1994 to 1999 and bottom topography along 145°W.

description of eddies in the central Gulf of Alaska using recent hydrographic data.

Data and bottom topography of the region

Hydrographic measurements using a CTD (Neil Brown Mark 3B, Accuracy of temperature: ± 0.005°C, salinity: ± 0.006 psu, pressure: ± 3.2db) were carried out every June-July from 1994 to 1999 by the T.S. Oshoro-Maru of the Faculty of Fisheries, Hokkaido University. CTD stations were set along the 145°W meridian, which passes across several seamounts (Fig. 2). Profiles were made for potential temperature, salinity and geostrophic velocity referred to 3,000 m or the bottom for each year. Volume transports (referred to 3,000 m or the bottom) were calculated for the intervals between each CTD station.

The abyssal plain in the Northeast Pacific ranges 3,000 to 5,000 m in depth and gradually deepens towards the central North Pacific (Fig. 3). The Aleutian Trench

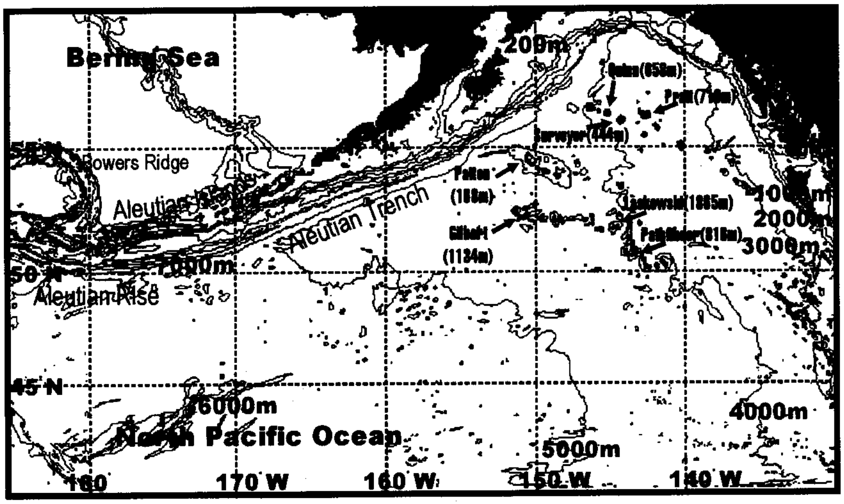

Fig. 3. Bathymetric map of the eastern North Pacific from GEBCO-97 digital atlas.

is located south and parallel to the Aleutian Islands. The continental shelf along the south coast of the Gulf of Alaska and Alaska Peninsula is relatively wide, but along the west coast of the Gulf of Alaska and Aleutian Islands, it is very narrow. Within the Gulf of Alaska, there are a number of seamounts and guyots that rise abruptly from the seafloor. Between 140°W and 150°W west of Sitka (Fig. 1), there are three seamounts (Surveyor, Quinn and Pratt). The present transect crossed the Quinn Seamount at 56°20′N.

Results

Temperature and salinity sections along 145° W

Vertical sections of potential temperature and salinity with bottom topography along 145°W are shown in Fig. 4 and Fig. 5, respectively. A Strong frontal structure was not recognized in either section for all years. From 1995 to 1997, when the observation lines extended nearshore, warm and less saline water occurred in the surface layer north of 57°N. This less dense water deepened the isopleths towards to north, even in deep layers. This deep baroclinic structure caused a westward geostrophic flow (Fig. 6), which is the Alaskan Stream. In 1995, a warm core occurred at 100–300 m layer, and a halocline depression was recognized near 56°20′ N. Isopleth depressions of both temperature and salinity near 56°20′N occurred to at least 2,000 m and extended to the peak of the Quinn Seamount. These features indicate the existence of a large baroclinic and anticyclonic eddy. In 1996 and 1997, no such structure was recognized.

In 1994, 1998 and 1999, when all stations were located south of 56°N, warm cores and isopleths depressions were recorded at the northern end of the transects. In 1994 and 1999, transects crossed the southern part of anticyclonic eddies as in 1995. Warm cores were also recognized in 1997 centered at 55°N and in 1998 centered at 52°30′N. However, these eddy features were limited to the surface layer above 1,000

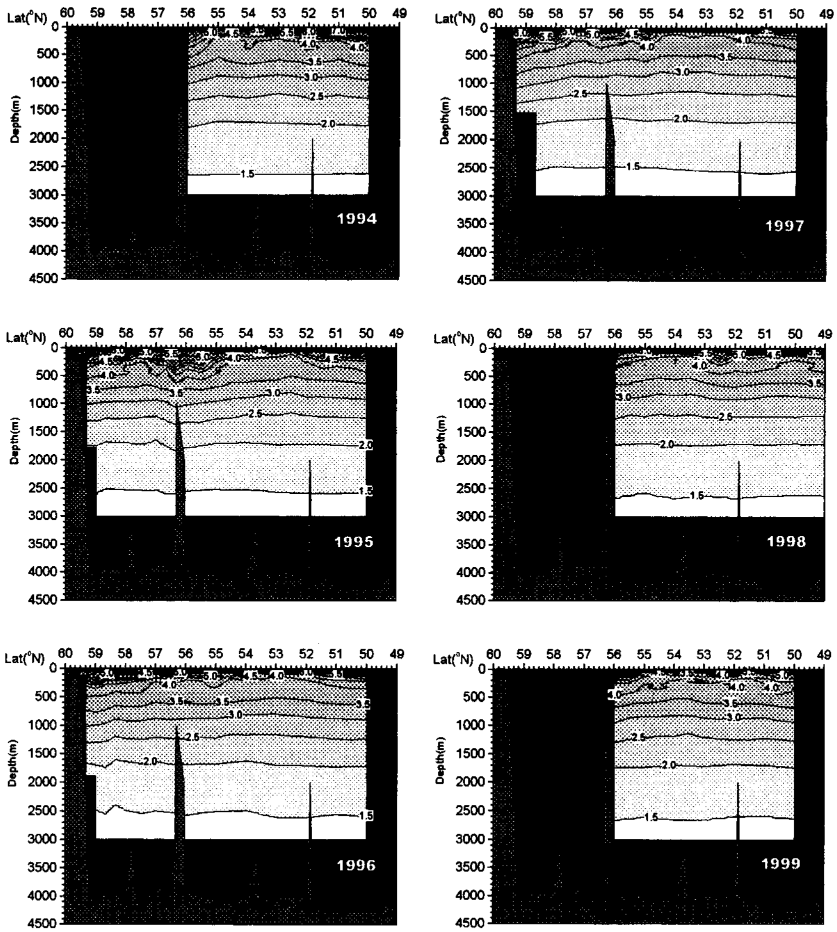

Fig. 4. Vertical distribution of potential temperature (°C) along 145°W from 1994 to 1999 with bottom topography.

m depth, and the horizontal scales (diameter is about 100 km) were smaller than for the eddies centered at the peak of the Quinn Seamount (diameter is over 200 km).

Geostrophic velocity structure and volume transport along 145° W

Geostrophic velocity structures (referred to 3,000 m depth or the seafloor) along 145°W each year are shown in Fig. 6. Flow never reached over 10 cm $\cdot$ s^{-1} south of 55°N in all years. From nearshore to 57°N, westward flow (the Alaskan Stream) was dominant in all years when the observation line extended nearshore. The net volume transport between 57°N and the northernmost stations was 7.5×10^6 $m^3 \cdot s^{-1}$ in 1995, 6.3×10^6 $m^3 \cdot s^{-1}$ in 1996 and 12.7×10^6 $m^3 \cdot s^{-1}$ in 1997 (Table 1). This annual variation of the volume transport in the Alaskan Stream is similar to the variation along 180° (21.8×10^6 $m^3 \cdot s^{-1}$, 22.4×10^6 $m^3 \cdot s^{-1}$ and 41.0×10^6 $m^3 \cdot s^{-1}$, respectively) reported by Onishi and Ohtani (1999). However, the net volume transport along 145°W was only about 1/3 of that along 180°.

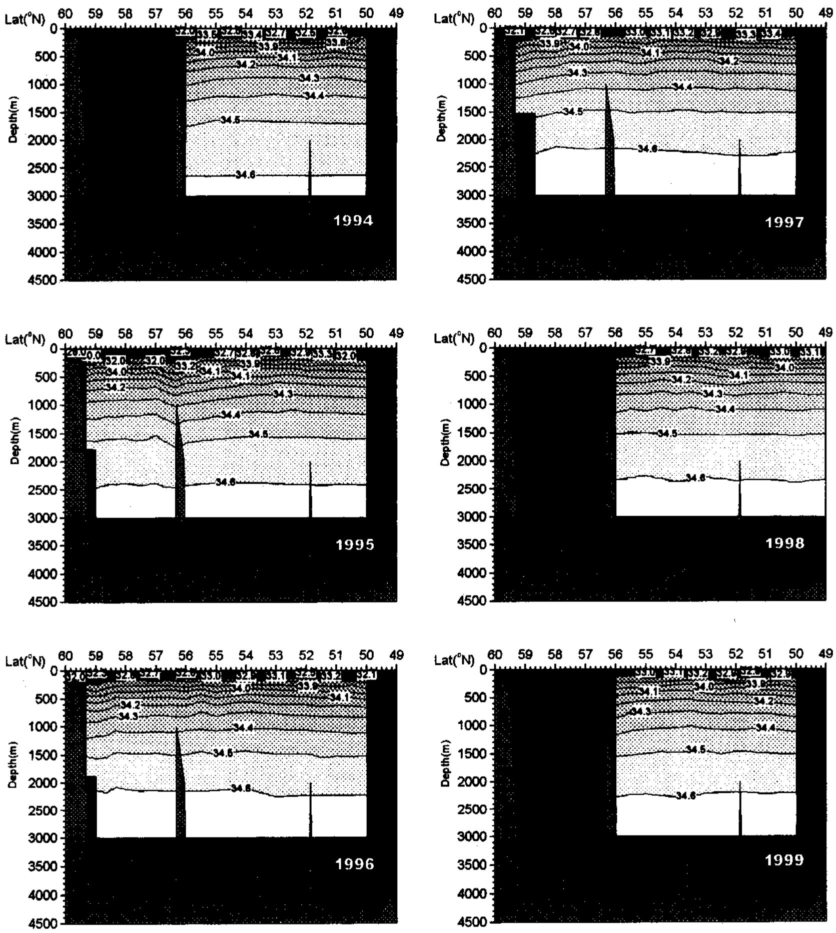

Fig. 5. Vertical distribution of salinity (psu) along 145°W from 1994 to 1999 with bottom topography.

In 1995 (Fig. 6), a strong eastward flow was observed north of Quinn Seamount, and a strong westward flow was observed south of the seamount. The maximum speed of the eastward flow was 30.3 cm • s^{-1} at the surface between 56°20′ and 56°40′ N. The maximum speed of the westward flow was 20.2 cm • s^{-1} at 150 m depth between 56°00′ and 56°20′N. The flow structure was very deep ; at 1,500 m depth, a 3.7 cm • s^{-1} eastward flow and a 3.3 cm • s^{-1} westward flow were observed in the two respective sections. The eastward flow was about 100 km wide, and the total eastward volume transport was 14.0×10^6 m^3 • s^{-1}. The westward flow was over 120 km wide. The total westward volume transport was 13.5×10^6 m^3 • s^{-1} in the three sections in which the maximum speed in the section was over 10 cm • s^{-1}. The eastward and westward total volume transports were similar. This anticyclonic eddy volume transport was larger than the volume transport in the Alaskan Stream in 1995. In 1994 and 1999, strong and deep westward flows were recognized in the north end sections. These structures may represent the southern parts of an anticy-

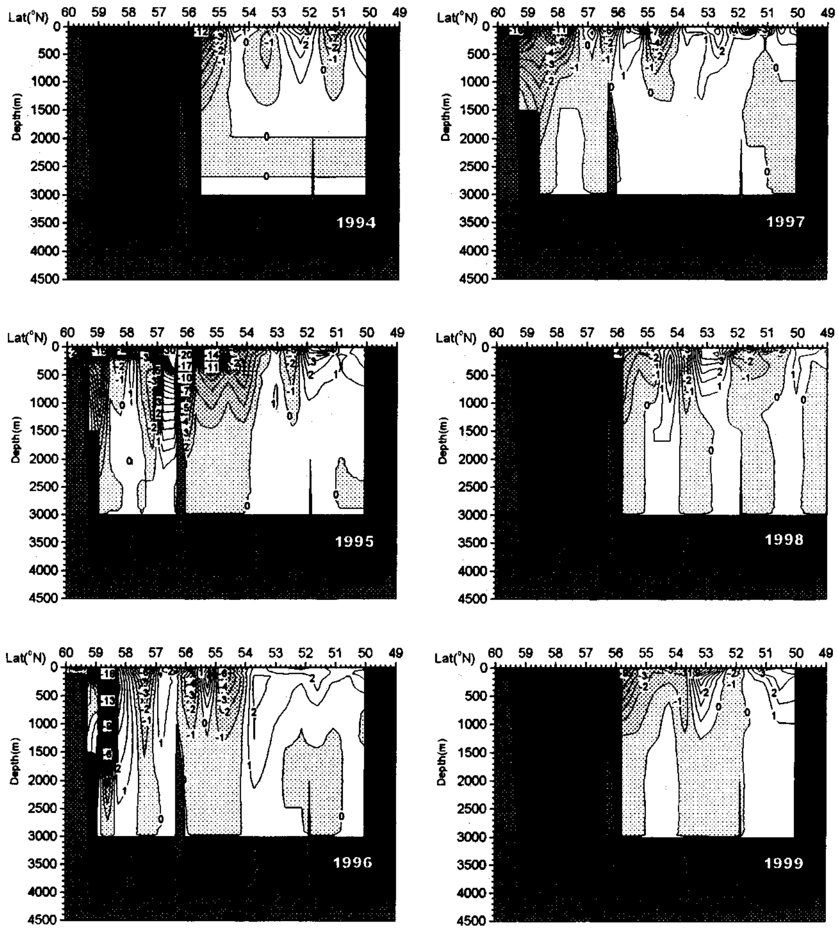

Fig. 6. Vertical distribution of geostrophic velocity (cm • s^{-1}) along 145°W from 1994 to 1999 with bottom topography. Shaded area (−) shows a westward flow.

clonic eddy, as in 1995.

Comparison of vertical structure between 1995 and 1997

To clarify the difference in vertical structure when a large eddy was present and when one was absent, potential temperature (Fig. 7) and salinity (Fig. 8) profiles at the same or closest position were compared between 1995 and 1997. Above the thermocline, temperatures were about 2°C warmer in 1997 than in 1995 at all stations, and the thermocline at about 40 m depth was stronger in 1997. Below the thermocline and in the halocline, a mesothermal layer (intermediate warm layer) occurred at several stations. At 59°20′N, which is the station closest to shore, a thick layer of low salinity water transported by the Alaskan Stream depressed the mesothermal layer to below 200 m depth in both 1995 and 1997. Towards the south (i.e. offshore), the layer of less saline water became thin, and the mesothermal layer ascended. At 57°40′N in 1995 and 57°30′N in 1997, the mesothermal structure was

Table 1. Volume transport in each section along 145°W from 1994 to 1999. (+) indicates an eastward transport, (−) indicates a westward transport.

Year	Section (Latitude N)	Volume Transport ($\times 10^6\ m^3 \cdot s^{-1}$)	Referrence Level
1994	56°00′-55°00′	−8.31	0-3,000/3,000 m
	55°00′-54°00′	1.42	0-3,000/3,000 m
	54°00′-53°00′	−2.52	0-3,000/3,000 m
	53°00′-52°00′	4.37	0-3,000/3,000 m
	52°00′-51°00′	−3.26	0-3,000/3,000 m
	51°00′-50°00′	4.56	0-3,000/3,000 m
1995	60°00′-59°40′	−0.11	0-100/100 m
	59°40′-59°20′	0.04	0-125/125 m
	59°20′-59°00′	−1.53	0-1,500/1,500 m
	59°00′-58°40′	−4.11	0-3,000/3,000 m
	58°40′-58°20′	0.00	0-3,000/3,000 m
	58°20′-58°00′	−0.94	0-3,000/3,000 m
	58°00′-57°40′	0.73	0-3,000/3,000 m
	57°40′-57°20′	−0.89	0-3,000/3,000 m
	57°20′-57°00′	−0.63	0-3,000/3,000 m
	57°00′-56°40′	6.00	0-3,000/3,000 m
	56°40′-56°20′	8.03	0-3,000/3,000 m
	56°20′-56°00′	−6.29	0-3,000/3,000 m
	56°00-55°30′	−1.95	0-3,000/3,000 m
	55°30′-55°00′	−5.25	0-3,000/3,000 m
	55°00′-54°30′	−1.33	0-3,000/3,000 m
	54°30′-54°00′	−2.79	0-3,000/3,000 m
	54°00′-53°30′	0.14	0-3,000/3,000 m
	53°30′-53°00′	0.97	0-3,000/3,000 m
	53°00′-52°30′	−1.61	0-3,000/3,000 m
	52°30′-52°00′	1.93	0-3,000/3,000 m
	52°00′-51°30′	1.47	0-3,000/3,000 m
	51°30′-50°45′	0.85	0-3,000/3,000 m
	50°45′-50°00′	1.65	0-3,000/3,000 m
1996	60°00′-59°40′	0.03	0-100/100 m
	59°40′-59°20′	−0.09	0-100/100 m
	59°20′-59°00′	0.34	0-1,500/1,500 m
	59°00′-58°40′	−0.23	0-3,000/3,000 m
	58°40′-58°20′	−8.44	0-3,000/3,000 m
	58°20′-58°00′	2.94	0-3,000/3,000 m
	58°00′-57°30′	1.81	0-3,000/3,000 m
	57°30′-57°00′	−2.69	0-3,000/3,000 m
	57°00′-56°30′	1.41	0-3,000/3,000 m
	56°30′-56°00′	0.72	0-3,000/3,000 m
	56°00′-55°30′	−2.13	0-3,000/3,000 m
	55°30′-55°00′	0.84	0-3,000/3,000 m
	55°00′-54°30′	−2.87	0-3,000/3,000 m
	54°30′-54°00′	−0.91	0-3,000/3,000 m
	54°00′-53°00′	4.80	0-3,000/3,000 m
	53°00′-52°30′	0.69	0-3,000/3,000 m
	52°30′-52°00′	0.43	0-3,000/3,000 m

	52°00′-51°30′	0.66	0-3,000/3,000 m
	51°30′-51°00′	0.26	0-3,000/3,000 m
	51°00′-50°30′	0.62	0-3,000/3,000 m
	50°30′-50°00′	0.57	0-3,000/3,000 m
1997	59°20′-58°40′	−4.56	0-1,500/1,500 m
	58°40′-58°00′	−4.97	0-3,000/3,000 m
	58°00′-57°30′	−2.42	0-3,000/3,000 m
	57°30′-57°00′	−0.73	0-3,000/3,000 m
	57°00′-56°30′	1.35	0-3,000/3,000 m
	56°30′-56°00′	−2.66	0-3,000/3,000 m
	56°00′-55°30′	1.35	0-3,000/3,000 m
	55°30′-55°00′	0.82	0-3,000/3,000 m
	55°00′-54°30′	−1.58	0-3,000/3,000 m
	54°30′-54°00′	−0.41	0-3,000/3,000 m
	54°00′-53°30′	0.49	0-3,000/3,000 m
	53°30′-53°00′	1.48	0-3,000/3,000 m
	53°00′-52°30′	1.81	0-3,000/3,000 m
	52°30′-52°00′	0.23	0-3,000/3,000 m
	52°00′-51°30′	0.14	0-3,000/3,000 m
	51°30′-51°00′	−0.06	0-3,000/3,000 m
	51°00′-50°30′	0.09	0-3,000/3,000 m
	50°30′-50°00′	−0.12	0-3,000/3,000 m
1998	56°00′-55°30′	−3.28	0-3,000/3,000 m
	55°30′-55°00′	−0.01	0-3,000/3,000 m
	55°00′-54°30′	−0.10	0-3,000/3,000 m
	54°30′-54°00′	2.51	0-3,000/3,000 m
	54°00′-53°30′	−1.89	0-3,000/3,000 m
	53°30′-53°00′	1.32	0-3,000/3,000 m
	53°00′-52°30′	2.32	0-3,000/3,000 m
	52°30′-52°00′	−0.70	0-3,000/3,000 m
	52°00′-51°30′	−1.25	0-3,000/3,000 m
	51°30′-51°00′	−0.16	0-3,000/3,000 m
	51°00′-50°30′	−0.14	0-3,000/3,000 m
	50°30′-50°00′	0.90	0-3,000/3,000 m
	50°00′-49°30′	−0.36	0-3,000/3,000 m
	49°30′-49°00′	−0.27	0-3,000/3,000 m
1999	56°00′-55°30′	−3.34	0-3,000/3,000 m
	55°30′-55°00′	−1.43	0-3,000/3,000 m
	55°00′-54°30′	−0.25	0-3,000/3,000 m
	54°30′-54°00′	−0.11	0-3,000/3,000 m
	54°00′-53°30′	−0.26	0-3,000/3,000 m
	53°30′-53°00′	0.67	0-3,000/3,000 m
	53°00′-52°30′	0.06	0-3,000/3,000 m
	52°30′-52°00′	−1.10	0-3,000/3,000 m
	52°00′-51°30′	−0.17	0-3,000/3,000 m
	51°30′-51°30′	1.23	0-3,000/3,000 m
	51°00′-50°30′	1.66	0-3,000/3,000 m
	50°30′-50°00′	1.49	0-3,000/3,000 m

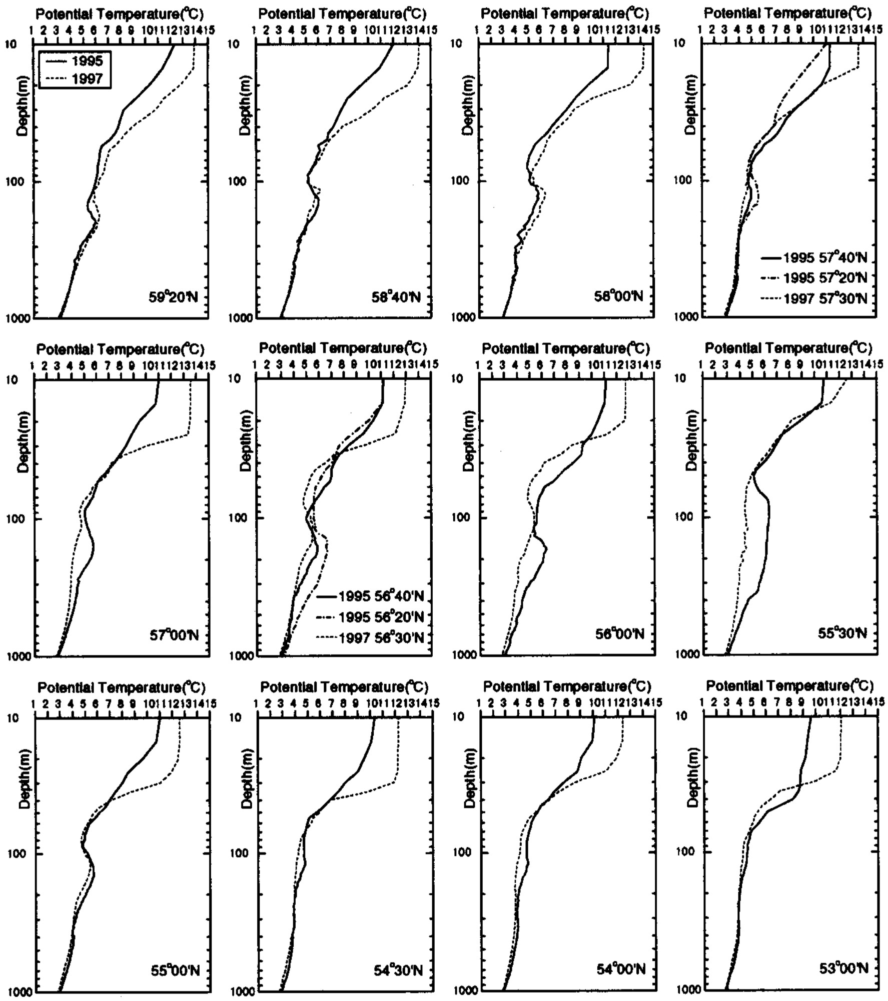

Fig. 7. Vertical profiles of potential temperature (°C) at each station along 145°W in 1995 and 1997.

almost absent. However, eddies brought the mesothermal structure to the offshore stations. As mentioned previously, there was a large anticyclonic eddy centered at 56°20′N in 1995. On the profile of temperature at 56°20′N in 1995, a deep (125–730 m), warm (maximum temperature : 6.6°C at 175 m) mesothermal layer was observed. At stations near the eddy's center (57°20′N–56°00′N), although the warm layer temperature was cooler and the layer depth was shallower, the mesothermal structure still remained. At 55°30′N in 1995, the mesothermal layer expanded and ascended, and the halocline depth ascended sharply. This expansion of the mesothermal layer is probably due to an overlap of the large eddy and small eddy. The small eddy centered at 55°30′N caused the mesothermal structure at 55°00′N. This structure occurred at 100–200 m depth, which is shallower than in the large eddy. The eastward flow north of this small eddy weakened the westward flow south of the

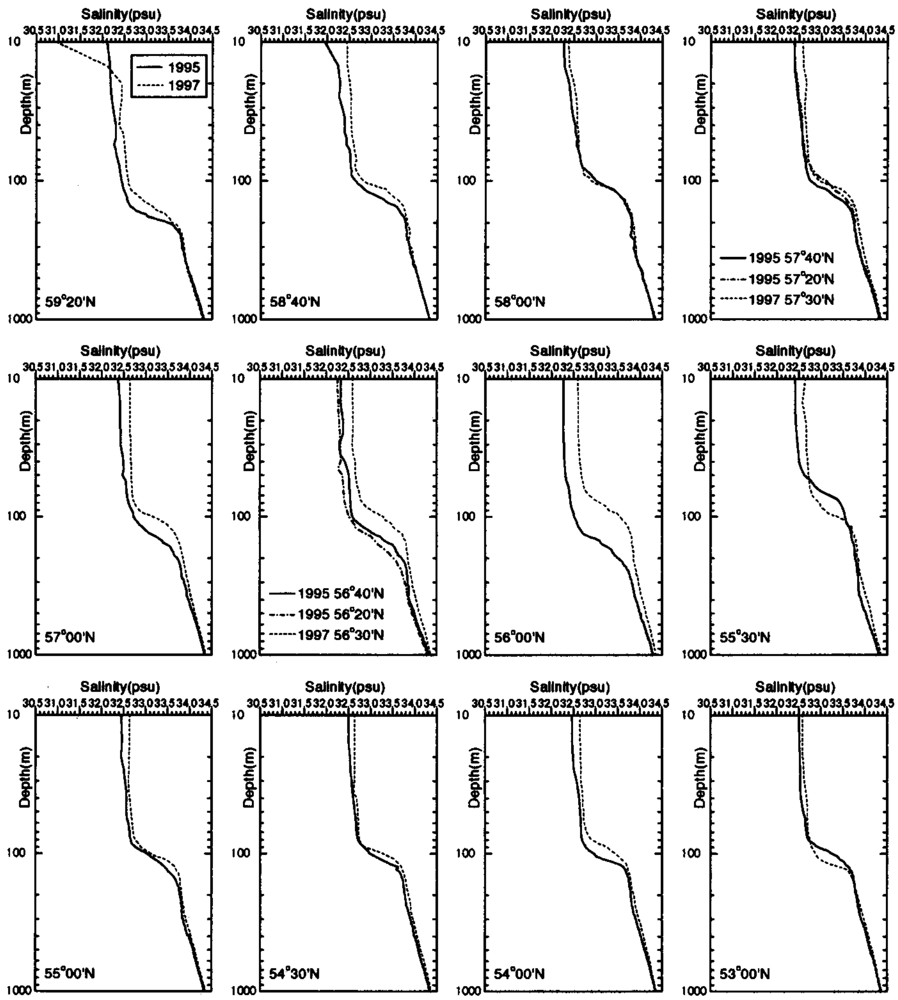

Fig. 8. Vertical profiles of salinity (psu) at each station along 145°W in 1995 and 1997.

large eddy. This effect can be recognized in the velocity section (Fig. 6) and volume transport (Table 1) in the section between 56°00′N and 55°30′N. In 1997, the mesothermal structure can be also found offshore (56°30′N, 56°00′N and 55°00′N). However, eddies that bring the mesothermal structures may be small, since these mesothermal layers in 1997 are shallower than in the large eddy in 1995. This difference is remarkable at 56°00′N. The coincidence of the temperature profiles in the mesothermal layer at 55°00′N indicates that eddies in 1997 were of the same scale as the small eddy in 1995. The Scales and distributions of these eddies can be ascertained by dynamic topography variations in Fig. 9.

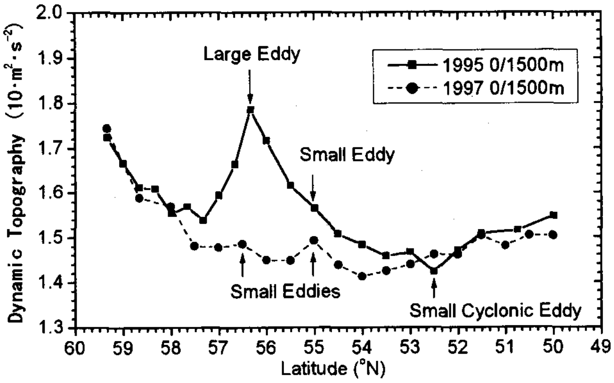

Fig. 9. Dynamic topography ($10 \cdot m^2 \cdot s^{-2}$) of surface referred to 1,500 m in 1995 and 1997 along 145°W.

Discussion and Summary

Several characteristics of anticyclonic eddies along 145°W were observed each summer from 1994 to 1999 (Table 2). Every year, there was a large and deep baroclinic eddy centered at 56°20′N above the Quinn Seamount. The particularly large eddy observed in 1995 is very similar to the Sitka Eddy reported by Tabata (1982), who described a baroclinic structure at depths over 2,000 m, a warm core at 100–200 m depth, a halocline depression, and a diameter of 200–300 km. The maximum volume transport on one side of the eddy was over $15 \times 10^6\ m^3 \cdot s^{-1}$ (0–2,000/2,000 db). Tabata (1982) noted that the eddy propagated westward as a planetary Rossby wave. Matthews et al. (1992) examined the westward propagation of the Sitka Eddy by local wind forcing from GEOSAT altimetry data. The large eddy observed in the present study was centered at 56°20′N, 145°00′W, which is west of Sitka (57°N, 135°W).

Several studies have indicated that mesoscale eddies can be generated in the open ocean by bottom topography. Bennett (1959) suggested that seamount chains in the Gulf of Alaska can produce considerable effects on ocean circulation. Using a numerical model, Huppert and Bryan (1976) verified that the cyclonic and anticyclonic vorticity distribution generated by flow over seamounts made the warm and cold eddies. Reed (1980) concluded that a clockwise eddy observed near the Surveyor Seamount (see Fig. 3) was induced by the bottom topography, based on the results of Huppert and Bryan (1976). However, according to the results of Huppert and Bryan (1976), a cyclonic eddy must be generated along with an anticyclonic eddy. In our results, no cyclonic eddies comparable in size to the large anticyclonic eddies were observed. A cyclonic eddy feature observed at 52°30′N in 1995 (Fig. 6 and 9) was comparable to the small anticyclonic eddies. Royer (1978) reported on small eddies (diameters of about 37 km) generated by seamounts in the North Pacific. Furthermore, water at the center of the large eddies was very similar to the coastal water in the Alaskan Stream. From these results, we suggest that the large anticyclonic eddies are brought by westward propagation of eddies generated in east coast of Alaska near Sitka. The deep baroclinic structure and large volume trans-

Table 2. Characteristics of physical properties of eddy along 145°W from 1994 to 1999. (+) indicates an eastward flow and transport, (−) indicates a westward flow and transport.

Year	Latiude of Eddy Center along 145°W	Horizontal Scale (Diameter, km)	Depth range of Mesothermal Layer (m)	Maximum Temperature in Mesothermal Layer (°C)	Depth of Halocline (m)	Maximum Velocity of Eddy ($cm \cdot s^{-1}$) (Refereed 3,000 m)	Volume Transport of Eddy ($\times 10^6 m^3 \cdot s^{-1}$) (0−3,000/3,000 m)	Rotation	Remarks
1994	56°00′N	220∼	70-500	6.3 (115m)	75	…/−12.1	…/−8.3	Anticyclonic	Entire Eddy not observed
	54°00′N	200	…	…	75	2.6/−1.5	1.4/−2.5	Anticyclonic	No Mesothermal layer
	52°00′N	200	…	…	110	6.2/−4.6	4.4/−3.3	Anticyclonic	No Mesothermal layer
1995	56°20′N	220	125-730	6.6 (175 m)	125	30.3/−20.2	14.0/−13.5	Anticyclonic	
	55°00′N	110	85-250	5.7 (140 m)	95	…/−8.5	…/−2.8	Anticyclonic	
	52°30′N	110	…	…	80	6.2/−6.4	1.9/−1.6	Cyclonic	No Mesothermal layer
1996	55°00′N	110	95-230	5.4 (120 m)	105	4.2/−6.2	0.8/−2.9	Anticyclonic	
1997	56°30′N	110	80-235	5.5 (115 m)	95	2.3/−5.8	1.4/−2.7	Anticyclonic	
	55°00′N	110	85-245	5.4 (130 m)	105	7.0/−7.7	0.8/−1.6	Anticyclonic	
1998	56°00′N	220∼	75-270	5.3 (115 m)	105	…/−4.8	…/−3.3	Anticyclonic	Entire Eddy not observed
	52°30′N	160	75-310	6.4 (100 m)	75	6.4/−6.1	3.6/−2.1	Anticyclonic	
1999	56°00′N	330∼	65-280	6.4 (115 m)	70	…/−9.6	…/−5.0	Anticyclonic	Entire Eddy not observed

port of these eddies considerably affect circulation, and also presumably affect primary production and fisheries in the Gulf of Alaska.

Acknowledgements

We thank the officers and crew of the T.S. Oshoro-Maru, the members of the scientific parties and the Special Navigation Course Cadets for their generous and helpful support during the cruises. We also thank Drs. H. Miyake and M.J. Kishi, Hokkaido Univ., for their helpful discussions and Dr. J.R. Bower, for proofreading our manuscript.

References

Bennett, E.B. (1959). Some Oceanographic Features of the Northeast Pacific Ocean during August 1955. *J. Fish. Res. Bd. Canada*, **16**, 565-633.

Dodimead, A.J., F. Favorite and T. Hirano (1963). Salmon of the North Pacific Ocean-II, Review of Oceanography of the Subarctic Pacific region. *Bull. Int. North Pacific Fish. Comm.*, **13**, 1-195.

Faculty of Fisheries, Hokkaido Univ. (1995-1999). *Data Record of Exploratory Fishing.* Nos. **38**-**42**, Hokkaido Univ., Hakodate.

Favorite, F., A.J. Dodimead and K. Nasu (1976). Oceanography of the Subarctic Pacific region. *Bull. Int. North Pacific Fish. Comm.*, **33**, 1-187.

Huppert, H.E. and K. Bryan (1976). Topographically generated eddies. *Deep-Sea Res.*, **23**, 655-679.

Matthews, P.E., M.A. Johnson and J.J. O'Brien (1992). Observation of Mesoscale Ocean Features in the Northeast Pacific Using Geosat Radar Altimetry Data. *J. Geophys. Res.*, **97**, 17829-17840.

Meyers, S.D. and S. Basu (1999). Eddies in the eastern Gulf of Alaska from TOPEX/POSEIDON altimetry. *J. Geophys. Res.*, **104**, 13333-13343.

Onishi, H. and K. Ohtani (1999). On Seasonal and Year to Year Variation in Flow of the Alaskan Stream in the Central North Pacific. *J. Oceanogr.*, **55**, 597-608.

Reed, R.K. (1980). Recent Observations of a Large Eddy in the Gulf of Alaska. *Mar. Fish. Rev.*, (June), 29-31.

Royer, T.C. (1978). Ocean Eddies Generated by Seamounts in the North Pacific. *Science*, **199**, 1063-1064.

Tabata, S. (1982). The Anticyclonic Eddy off Sitka, Alaska, in the Northeast Pacific Ocean. *J. Phys. Oceanogr.*, **12**, 1260-1282.

Thomson, R.E. and J.F.R. Gower (1998). A basin-scale oceanic instability event in the Gulf of Alaska. *J. Geophys. Res.*, **103**, 3033-3040.

Uda, M. (1963). Oceanography of the Subarctic Pacific Ocean. *J. Fish. Res. Bd. Canada*, **20**, 119-179.